Domain structure investigation of non-stoichiometric strontium ferrites and cobaltites

Ancharova U. V.[*1], Cherepanova S.V.[2]

[1]Institute of Solid State Chemistry and Mechanochemistry SB RAS, Novosibirsk, Russia
[2]Boreskov Institute of Catalysis SB RAS, Novosibirsk, Russia
e-mail: ancharova@gmail.com

Monte Carlo domain structure simulation and Debye equation calculation of XRD patterns were used to confirm the formation of domain structure and investigate its peculiarities. Correspondence of simulated XRD patterns with synchrotron powder diffraction experiments is achieved on the conditions that beside of 90^o rotations of brownmillerite-like domains inside perovskite-like matrix each domain contains areas with perpendicularly oriented tetrahedral chains. Influence of such parameters as stoichiometry, average domain size, orthorhombic distortion degree on the XRD patterns is considered.

Key words: perovskite, brownmillerite, nonstoichiometry, domain structure, simulation

I. INTRODUCTION

High-temperature modifications of strontium ferrites and cobaltites have cubic perovskite $ABO_{3-\delta}$ structure with $Pm\bar{3}m$ space group. Oxygen vacancies which can present in perovskite structure are statistically distributed and don't disturb its cubic symmetry. Cooling to ambient temperatures leads to the vacancy ordering and the formation of vacancy ordered phases. Depending on the non-stoichiometry of low-temperature phase $ABO_{3-\delta}$, it is possible the formation of stoichiometric perovskite-related $ABO_{2.5}$, $ABO_{2.75}$, $ABO_{2.875}$ phases (Takeda *et al.*, 1986; Hodges *et al.*, 2000; Le Toquin *et al.*, 2006).

HRTEM studies of many nonstoichiometric cation modified perovskite-like compounds $ABO_{3-\delta}$ with stoichiometry close to brownmillerite-like $ABO_{2.5}$ show (Nakayama *et al.*, 1987; Lindberg *et al.*, 2004; Doorn and Burggraaf, 2000; Liu *et al.*, 2003; Alario-Franco *et al.*, 1982; D'Hondt *et al.*, 2009) that the crystals contain perpendicular oriented brownmillerite microdomains, which are intergrown three-dimensionally with the parent perovskite structure.

The crystal structure of brownmillerite $ABO_{2.5}$ is related to the perovskite ABO_3 one. The ideal perovskite structure consists of layers of corner sharing BO_6-octahedra with A-cations in between. The brownmillerite structure can be described as a perovskite structure with one-sixth of the anion sites vacant. The oxygen vacancies ordering lead to a structure which is composed of alternating layers (perpendicular to the b_{BM}-axis) of corner sharing BO_6-octahedra and BO_4-tetrahedra zigzagly arranged along the c_{BM}-axis. The resulting unit cell is orthorhombic with $a_{BM} \approx a_{per}\sqrt{2}$, $b_{BM} \approx 4a_{per}$, $c_{BM} \approx a_{per}\sqrt{2}$. The B and O atoms in the BO_4 layers are displaced from their ideal octahedral positions in the perovskite structure. This displacement can be described as a cooperative rotation of the BO_4 tetrahedra in the chains. Orthorhombic distortions lead to the deformation of vacancy-ordered brownmillerite structure relative to the parent perovskite structure.

Formation of the domain structure for $ABO_{2.5+x}$ is energetically favorable process since different orientations of domains minimize the total energy of deformation fields in the crystal. At the same time the domain partition leads to the increase of the domain-wall energy. The balance of this counteracting factors defines the system state in which long range order parameter is characterized by the equilibrium value of the average domain size, which can be estimated from the HRTEM data as ~10nm (Nakayama *et al.*, 1987; Lindberg *et al.*, 2004). Superstoichiometric

https://doi.org/10.1017/S0885715613001152 Published online by Cambridge University Press

oxygen *x* is localized at the domain walls and prevents further growth of domains (Nakayama *et al.*, 1987).

Compounds which have microdomain structure (according to HRTEM) show definite XRD patterns (Nakayama *et al.*, 1987; Hodges *et al.*, 2000; Lindberg *et al.*, 2004). Despite the orthorhombic symmetry within each domain the peaks corresponding to the high-symmetric cubic perovskite structure are observed. But along with these intensive narrow peaks the additional weak broadened peaks are also observed. Taking into account that HRTEM is a good tool for the investigation of local structure only and that this method is largely two-dimensional we have used a Monte-Carlo microstructure simulation accompanied by the calculation of the corresponding X-ray diffraction profiles. The aim of this work is to show that such specific XRD patterns related to the average structure are characteristic for the microdomain structure of non-stoichiometric perovskite-like compounds with stoichiometry close to brownmillerite-like.

II. EXPERIMENTAL

The samples were prepared by the standard ceramic method using as precursors $SrCO_3$, Fe_2O_3, Co_3O_4 (and other metal oxides for cation modification) of analytical or reagent grade. Appropriate mixtures of strontium carbonate and oxides were ground in an AGO-2 planetary ball mill at 20g, calcined at 900°C for 6 h and pressed into disks, which were fired in air at temperatures from 1200 to 1300°C for 6 h. In order to decrease the oxygen stoichiometry the cation-substituted samples were annealed at ~900ºC in vacuum ~10^3 Pa and then quenched in vacuum to the room temperature. The sample of $SrCo_{0.8}Fe_{0.2}O_{2.64}$ was used as-sintered, because quenching in vacuum of this compound leads to the formation of the brownmillerite structure. The oxygen content in the samples was measured by means of iodometric titration (Weiss, 1998).

The XRD experiments were performed with use of synchrotron radiation (SR) at the fourth beamline (Ancharov *et al.*, 2001) of the VEPP-3 storage ring, Siberian Synchrotron and Terahertz Radiation Center (Budker Institute of Nuclear Physics, Novosibirsk, Russia). The SR beam generated by the wiggler magnet was monochromated by the single reflection from the crystal-monochromator Si(111) in Laue geometry to the wavelength of 0.369 Å ($\Delta\lambda/\lambda$~10^{-3}) and was diffracted by the sample in Debye-Scherrer geometry. The scattering intensity was gathered by 2D image plate detector mar345 and integrated over azimuth angle in order to obtain the dependence of the scattering intensity on the angle 2θ.

https://doi.org/10.1017/S0885715613001152 Published online by Cambridge University Press

The full-profile Rietveld analysis of XRD patterns was performed with use of PowderCell software. Monte Carlo simulation of the particles having domain structure and Debye equation calculation of the diffracted intensities on the generated particles were made with use of DISCUS program package (Proffen and Neder, 1997). The visualization of structure was made with use of computer program Vesta 3 (Momma and Izumi, 2011).

III. RESULTS AND DISCUSSION

It was found that X-ray diffraction for $SrFe_{0.94}Mo_{0.06}O_{2.66}$, $SrCo_{0.8}Fe_{0.2}O_{2.64}$ and $Sr_{0.7}La_{0.3}Co_{0.5}Al_{0.3}Fe_{0.2}O_{2.54}$ have common features (Figure 1). One can see that all XRD patterns contain intensive narrow peaks corresponding to the perovskite structure with $Pm\bar{3}m$ symmetry and additional weak broadened ones ($\leqslant$2% of the strongest peak). Widths of all peaks are shown in the inset to Figure 1. All peaks can be indexed in the doubled cubic perovskite unit cell with lattice constants $a = b = a_{per}$ and $c = 2a_{per}$. Electron diffraction also shows the reflections with half-integer indexes (Ancharova *et al.*, 2012).

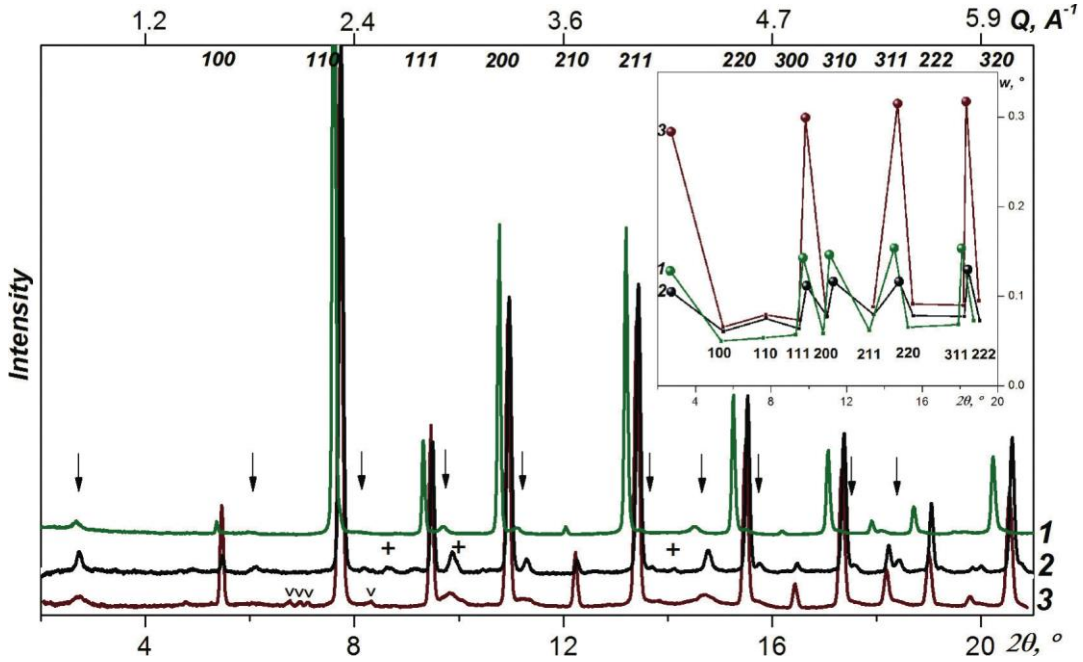

Figure 1**.** Powder diffraction patterns of nonstoichiometric perovskite-like oxides with superstructure reflections (↓; ●), λ = 0.369 Å: (1) $SrFe_{0.94}Mo_{0.06}O_{2.66}$; (2) $SrCo_{0.8}Fe_{0.2}O_{2.64}$; sign (+) marks the ~0.5% of CoO phase; (3) $Sr_{0.7}La_{0.3}Co_{0.5}Al_{0.3}Fe_{0.2}O_{2.54}$; sign (v) marks the ~1% of $SrAl_2O_4$ phase; (inset): widths of the diffraction maxima, depending on the composition (1-3).

Mössbauer spectroscopy investigation of $SrFe_{0.95}Mo_{0.05}O_{2.66}$ carried out earlier (Markov *et al.*, 2009) showed that along with octahedral coordination of Fe^{3+} cations (63%) there are

https://doi.org/10.1017/S0885715613001152 Published online by Cambridge University Press

tetrahedral coordinated ones (37%) that can be interpreted as coexistence of perovskite and brownmillerite structures in the 41:59 ratio respectively. HRTEM image of $SrFe_{0.95}Mo_{0.05}O_{2.66}$ indicates domain structure consisting of coherently stacked brownmillerite-like blocks perpendicular to each other (Figure 2).

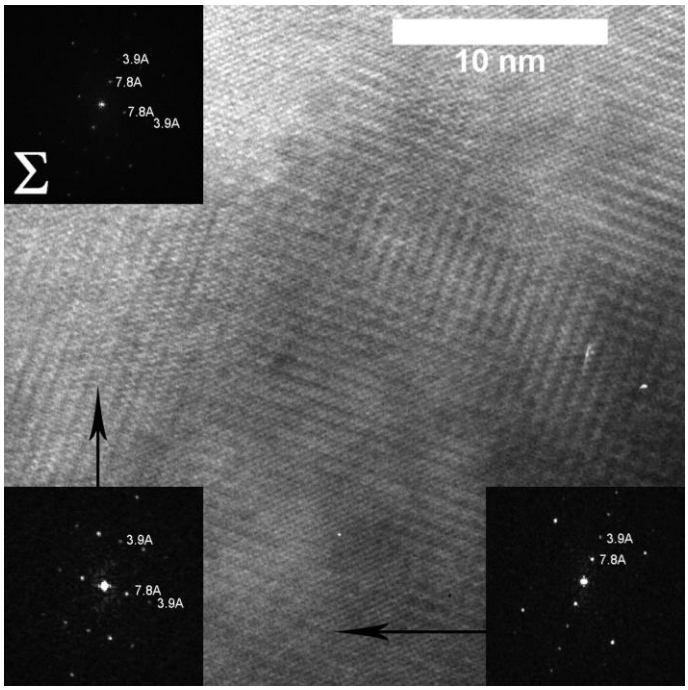

Figure 2. The HRTEM image of $SrFe_{0.95}Mo_{0.05}O_{2.66}$ and fast Fourier transform of perpendicularly oriented fragments with the brownmillerite structure (bottom); FFT of average domain orientations (top).

Evidently that full profile Rietveld analysis developed for the perfect crystals is not suitable in this case due to disturbance of three-dimensional order. Its formal application for the $SrFe_{0.94}Mo_{0.06}O_{2.66}$ and $SrCo_{0.8}Fe_{0.2}O_{2.64}$ XRD patterns (Figures 3(a) and 3(b)) give good values of *R*-factor (~3.5-4%) for the mixture of perovskite- and brownmillerite-like phases but with unrealistic brownmillerite lattice constants equal to each other $a_{BM}/\sqrt{2} = b_{BM}/4 = c_{BM}/\sqrt{2}$ and to a_{per}.

It is not possible to fit simultaneously widths of narrow main peaks and broad superstructure ones (inset to Figure 1) with use of Rietveld method. Also one can see excess peaks on the simulated XRD patterns (Figures 3(a) and 3(b)). So further investigation was carried out by Monte-Carlo simulation of particles having domain structure and Debye equation calculation of diffracted intensities on the generated particles. This approach makes it possible to study the diffraction effects on the materials that have any structure and condition of 3D periodicity is not obligatory.

https://doi.org/10.1017/S0885715613001152 Published online by Cambridge University Press

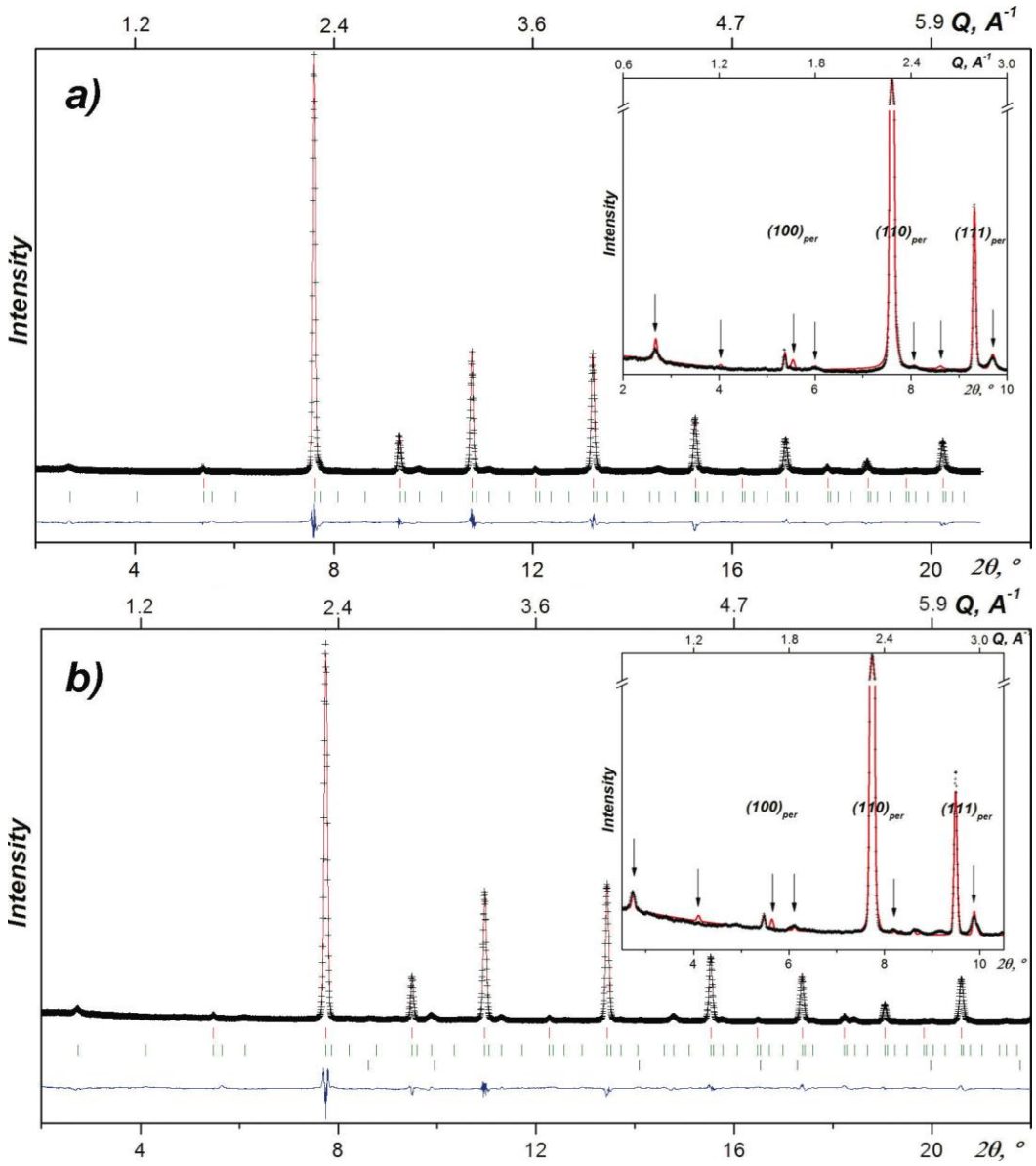

Figure 3. The full-profile Rietveld refinements of the experimental X-Ray powder diffraction patterns for (a) $SrFe_{0.94}Mo_{0.06}O_{2.66}$, a_{per} = 3.923 Å by two-phase system: 79% ABO_3 (perovskite structure) + 21% $ABO_{2.5}$ (brownmillerite structure, $a_{BM}=2^{½}\cdot a_{per}$, $b_{BM}=4\cdot a_{per}$, $c_{BM}=2^{½}\cdot a_{per}$), R_p = 4%; (b) $SrCo_{0.8}Fe_{0.2}O_{2.64}$, a_{per} = 3.856 Å by three-phase system: 71% ABO_3 (perovskite structure) + 29% $ABO_{2.5}$ (brownmillerite structure, $a_{BM}=2^{½}\cdot a_{per}$, $b_{BM}=4\cdot a_{per}$, $c_{BM}=2^{½}\cdot a_{per}$) + 0.5% CoO, R_p = 3.5%, λ = 0.369 Å.

A. Monte-Carlo simulation of domain structure

For Monte-Carlo simulation of domain structure the cluster-variation-method was used in the binary alloy model. To generate particles consisting of brownmillerite microdomains, which are intergrown three-dimensionally with the parent perovskite structure, at the first stage four types of clusters are randomly distributed in the 3D matrix of N^3=20×20×20 size. Probability of perovskite-like clusters P_{per} is determined by oxygen excess x in $ABO_{2.5+x}$. Brownmillerite type

https://doi.org/10.1017/S0885715613001152 Published online by Cambridge University Press

clusters with three orientations have equal probability $(1-P_{per})/3$. For close packing without free volume all types of clusters should have cubic shape of the same size. So cube with the edge equal to maximal lattice constant $b_{BM} \sim 4a_{per}$ has been chosen. Such cluster contains 64 perovskite- or 8 brownmillerite-like unit cells.

It is known that brownmillerite unit cell axes a_{BM} and c_{BM} approximately correspond to the face diagonals of the perovskite unit cell. So for the coherent connection of brownmillerite- and perovskite-like clusters the atomic coordinates in brownmillerite-like unit cell should be converted by the rotation of a_{BM} and c_{BM} axes around b_{BM} one by ~45° and multiplied to 16-fold perovskite unit cell $2a_{per}$x$4a_{per}$x$2a_{per}$ (Figure 4). Then atomic coordinates in this unit cell is multiplied to cluster size.

Cluster sorting has been made in the Monte Carlo technique by switching in positions of randomly selected pairs of clusters, depending on the desired parameters of the short and long range order. In the sorting process the clusters with the perovskite structure, which is the matrix of the host lattice, are displaced to the boundaries of domains with the brownmillerite structure.

The orthorhombic distortion of brownmillerite unit cell $a_{BM} \approx a_{per}\sqrt{2}$, $b_{BM} \approx 4a_{per}$, $c_{BM} \approx a_{per}\sqrt{2}$ leads to the distortion of brownmillerite-like cubic clusters (equal edges $a=b=c=4a_{per}$) into parallelepipeds with edges $a=c=2\sqrt{{a_{BM}}^2+{c_{BM}}^2} \neq b=b_{BM}$. Two cluster angles α and γ remain rectangular but the third one $\beta = 2arctg\left(a_{BM}/c_{BM}\right)$ is not equal to 90° (Figure 4). The lattice is distorted with the conservation of the unit cell volume. The orthorhombic distortion ε was determined as $\varepsilon = \left|\frac{b-4a_{per}}{4a_{per}}\right| = \left|\frac{(4a_{per})^2-ac}{ac}\right|$. For brownmillerite structures the values ε change from 0.5 to 1%.

https://doi.org/10.1017/S0885715613001152 Published online by Cambridge University Press

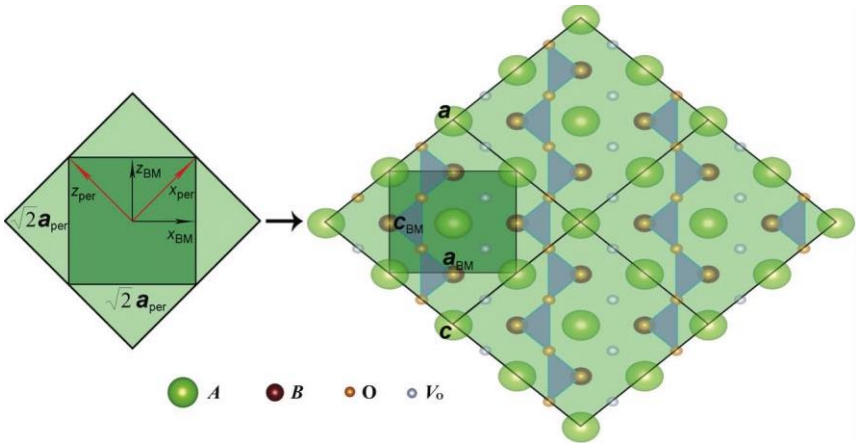

Figure 4. A schematic (0*k*0) cross-sections, illustrating (I) correspondence between brownmillerite axes a_{BM} and c_{BM} and perovskite unit cell doubled in two directions x_{per} and z_{per}; (II) the choice of the elementary cluster size for domain structure simulations and orthorhombic deformations in different coordinate systems (perovskite and brownmillerite).

The orthorombic distortion of brownmillerite unit cell leads to the shifts of the clusters relative to the matrix with cubic cells. These displacements were carried out with use of Monte Carlo technique with energy minimization. For this purpose the Lennard-Jones potential for the bond lengths and the harmonically potential for the bond angles were used.

From the viewpoint of the minimization of the total energy of deformation fields arising as result of orthorhombic distortions, formation of nanodomain structure is energetically favorable process. In (Grenier, *at al.*, 1985) it was offered the approach determining the mechanism of stress relaxation by the appearance of areas with perpendicularly oriented tetrahedra chains. This can be achieved not only by rotation of b_{BM} axis in three directions, but also by the 90° rotation of brownmillerite unit cell around b_{BM} axes or inversion of a_{BM} and c_{BM} axes.

B. Calculation of XRD patterns with use of the Debye equation

Real particle size is more then 100 nm. As consequence width of the main narrow peaks on the experimental and calculated XRD patterns is determined preferably by the width of instrumental function (~0.06-0.07°). The size of the simulated particles L is defined as $N4a_{per}$ ~30 nm is much smaller then real one. Scherrer dependence of peak width $B \sim \lambda / L\cos\theta$ in the small angle range (<20°) give almost constant value B=0.07°-0.08°. So this broadening on the calculated XRD patterns can be considered as analogue of instrumental one.

On the Figure 5 there are experimental XRD pattern for $SrFe_{0.94}Mo_{0.06}O_{2.66}$ and XRD patterns calculated for the four models: monodomain brownmillerite-like particles (model 1),

https://doi.org/10.1017/S0885715613001152 Published online by Cambridge University Press

brownmillerite-like particles containing areas with perpendicularly oriented tetrahedra chains (model 2), particles consisting of perpendicularly oriented brownmillerite-like domains in perovskite-like matrix (model 3), combination of the second and third models (model 4). In all cases the average domain size $\langle D \rangle$ was equal to ~9 nm, orthorhombic distortion ε was ~0.5%, oxygen stoicheometry 2.5+x was 2.52. There is significant difference between XRD patterns calculated for the models 2 and 3. Model 2 partially removes and model 3 fully removes orthorhombic splitting. Beside this the main diffraction effects for the model 2 and 3 are disappearance of excess peaks and broadening of superstructure peaks respectively. The combination of these two models (model 4) gives all desired diffraction effects. It represents perpendicularly oriented brownmillerite-like domains in perovskite-like matrix, where each domain is also disordered by 90° rotations of tetrahedra chains. The best correspondence gives the fifth model similar to the forth one but with oxygen stoichiometry (content of the perovskite clusters) close to one in $SrFe_{0.94}Mo_{0.06}O_{2.66}$.

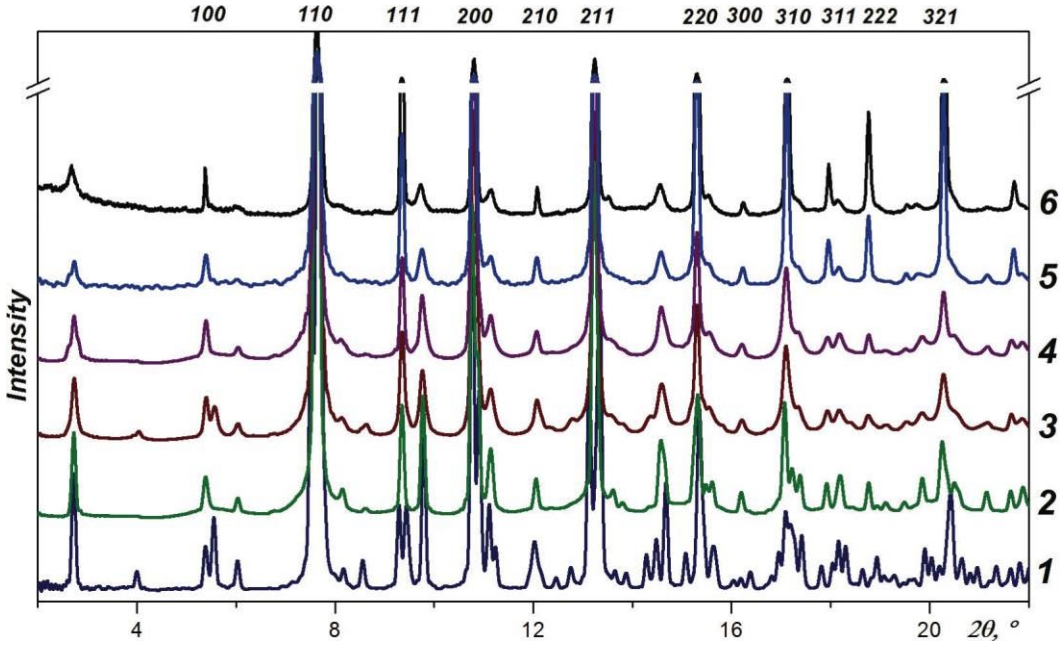

Figure 5. Calculated (1-5) and experimental (6) powder diffraction patterns of $SrFe_{0.94}Mo_{0.06}O_{2.5+x}$ for the different models: (1) mono-domain brownmillerite structure $ABO_{2.5}$; (2) the model of perpendicular-oriented tetrahedra chains in the brownmillerite structure, x=0.02; (3) the model of coherent-stacked perpendicular-oriented brownmillerite domains, x=0.02; (4-5) the models of formation of clusters with two possible tetrahedra-chain orientations inside each of the perpendicular-oriented brownmillerite domains: (4) x=0.02; (5) x=0.2; the indexes of diffraction maxima are given for the perovskite structure, λ = 0.369 Å.

https://doi.org/10.1017/S0885715613001152 Published online by Cambridge University Press

1. Influence of the ratio of brownmillerite- and perovskite-like clusters

This ratio is determined by oxygen excess x in $ABO_{2.5+x}$. The calculations of XRD patterns for different values of oxygen content $2.5+x$ from 2.52 to 2.75 in $SrCo_{0.8}Fe_{0.2}O_{2.5+x}$ show (Figure 6) expected result that increase in oxygen content leads to the decrease of the intensities of the superstructure peaks. Figure 6 also shows that the best correspondence with experimental XRD pattern for $SrCo_{0.8}Fe_{0.2}O_{2.64}$ is achieved just at $2.5+x=2.64$.

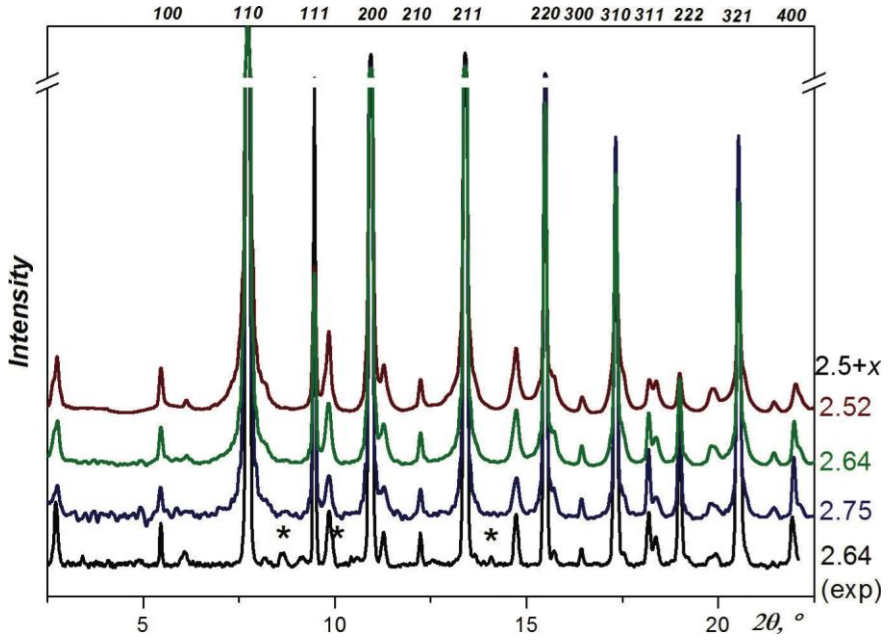

Figure 6. Experimental (bottom) and calculated powder diffraction patterns of $SrCo_{0.8}Fe_{0.2}O_{2.5+x}$ for the model of formation of clusters with two possible tetrahedra-chain orientations inside each of the perpendicular-oriented brownmillerite domains with $2.5+x$ = 2.75; 2.64; 2.52; sign (*) marks the CoO phase, λ = 0.369 Å.

2. Influence of the domain size

The calculations of the XRD patterns for the particles of the same size (~30 nm) but with different average domain size $\langle D \rangle$ from 2 to 13 nm without orthorhombic distortions show (Figure 7**)** that increasing in the domain size increases the intensities of the superstructure peaks. At the same time the widths of the main and additional peaks do not change in general. Increasing in intensities of the superstructure reflections can be connected with increasing in degree of long range order in the system.

https://doi.org/10.1017/S0885715613001152 Published online by Cambridge University Press

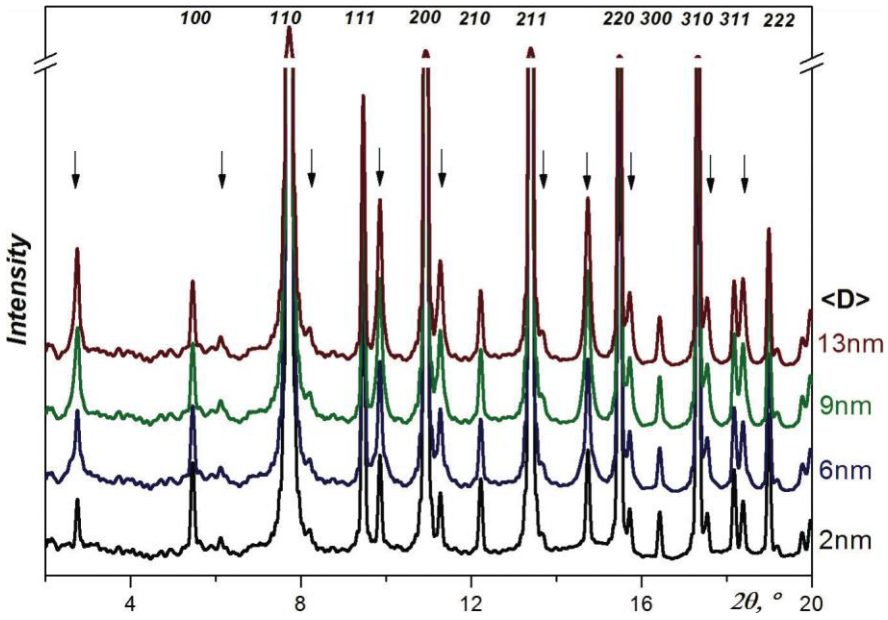

Figure 7. Powder diffraction patterns calculated for the composition $SrCo_{0.8}Fe_{0.2}O_{2.52}$ for systems of coherent-stacked brownmillerite domains (with two orientations of tetrahedra chains inside each of them) with different average domain size: 2, 6, 9, 13 nm.

3. Influence of the orthorhombic distortions

The calculations of XRD patterns with different orthorhombic distortions ε=0-1.5% show (Figure 8**)** that even in the absence of orthorhombic distortions (ε=0) the peaks additional for the perovskite structure are considerably broader than the main peaks. Increasing in orthorhombic distortion leads to further increasing in the widths of the superstructure peaks. At the same time widths of the main peaks remain. The superstructure peaks observed (Figure 1 inset) for the $Sr_{0.7}La_{0.3}Co_{0.5}Al_{0.3}Fe_{0.2}O_{2.54}$ are much broader as compared to the superstructure peaks for $SrFe_{0.94}Mo_{0.06}O_{2.66}$ and $SrCo_{0.8}Fe_{0.2}O_{2.64}$. It can be connected with high variance in cations sizes (~0.1Å) for the $Sr_{0.7}La_{0.3}Co_{0.5}Al_{0.3}Fe_{0.2}O_{2.54}$ system. For comparison this value is much smaller (~0.02Å) for $SrCo_{0.8}Fe_{0.2}O_{2.64}$ and $SrFe_{0.94}Mo_{0.06}O_{2.66}$. Probably higher variance in cations sizes causes stronger orthorhombic distortions.

https://doi.org/10.1017/S0885715613001152 Published online by Cambridge University Press

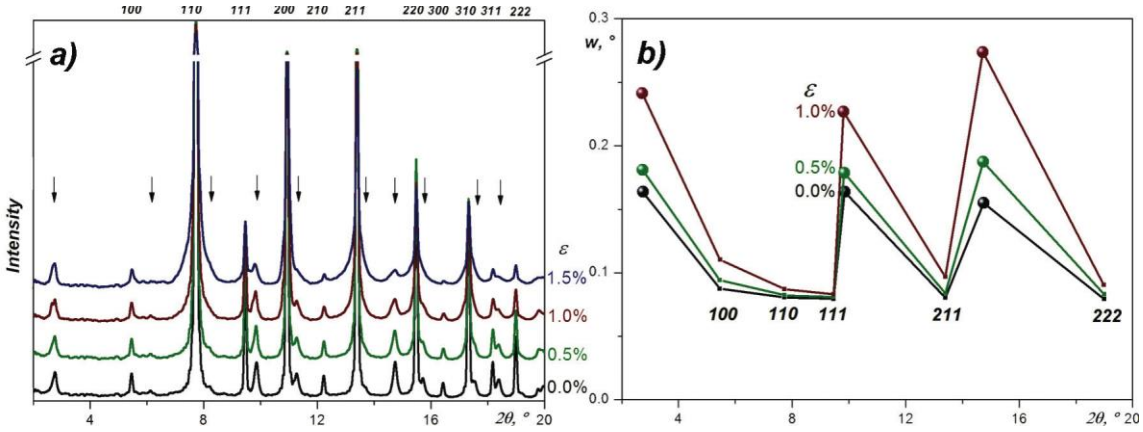

Figure 8. (a) powder diffraction patterns calculated for the $SrCo_{0.8}Fe_{0.2}O_{2.52}$ for systems of coherent-stacked brownmillerite domains (including perpendicular orientations of tetrahedra chains within) depending on values of orthorhombic strains within each of brownmillerite domains ε = 0; 0.5; 1; 1.5%; (b) widths of the diffraction maxima, depending on the strains (0; 0.5; 1%) obtained from corresponding diffraction profiles (a).

IV. CONCLUSION

Monte-Carlo simulations and Debye equation calculations of XRD patterns show that perovskite-like oxides with oxygen non-stoichiometry close to brownmillerite-like which XRD patterns are represented by the narrow intensive peaks corresponding to the cubic perovskite structure and by broad weak superstructure ones have microdomain structure. Domains have brownmillerite structure, rotated by 90^o relative to each other and coherently connected with parent perovskite matrix. Such domain structure model is characterized by the disappearance of the brownmillerite orthorhombic splitting and give narrow main peaks and broad superstructure peaks. XRD pattern calculated for this model is similar to the experimental ones but contains several excess peaks of low intensity. Only addition of 90^o rotation of tetrahedra chains inside each domain gives full correspondence with experiment. Also it was shown that the oxygen stoichiometry and the average domain size influent on the intensity of superstructure diffraction peaks. The widths of these peaks depend on the degree of the orthorhombic distortions.

V. ACKNOWLEDGMENTS

This work was carried out with use of equipment belonging to the shared research center "SSTRC" and supported by the Ministry of Education and Science of the Russian Federation.

Authors thank Gutakovsky A.K. for obtaining experimental data on the HRTEM.

https://doi.org/10.1017/S0885715613001152 Published online by Cambridge University Press

Alario-Franco, M. A., Joubert, J. C. and Lévy, J. P. (**1982**). "Anion deficiency in iron perovskites: The $Sr_xNd_{1-x}FeO_{3-y}$ solid solution I: 0.6<*x*<0.8," Mater. Res. Bull. **17**, 733-740.

Anderson, J. S. (**1970**). *Problems of Nonstoichiometry* (Amsterdam: North-Holland).

Ancharov, A. I., Manakov, A. Yu., Mezentsev, N. A., Tolochko, B. P., Sheromov, M. A. and Tsukanov, V. M. (**2001)**. "New station at the 4th beamline of the VEPP-3 storage ring," Nucl. Instrum. Methods Phys. Res., Sect. A **470**, 80-83.

Ancharova, U. V., Cherepatova, S. V. and Lyakhov, N. Z. (**2012**). "Simulation of the X-Ray diffraction pattern of nano-structured $Sr(Fe,Co)O_{3-\delta}$," Chem. Sustainable Dev. (4), 395-403. [http://www.sibran.ru/en/journals/Hviur/ accessed 7 Jul 2013].

D'Hondt, H., Hadermann, J., Abakumov, A. M., Kalyuzhnaya, A. S., Rozova, M. G., Tsirlin, A. A., Nath, R., Tan, H., Verbeeck, J., Antipov, E. V. and Tendeloo, G. V. (**2009**). "Synthesis, crystal structure and magnetic properties of the $Sr_2Al_{0.78}Mn_{1.22}O_{5.2}$ anion-deficient layered perovskite," J. Solid State Chem. **182**, 356-363.

Doorn, R. H. E., Burggraaf, A. J. (**2000**). "Structural aspects of the ionic conductivity of $La_{1-x}Sr_xCoO_{3-\delta,}$" Solid State Ionics. **128**, 65-78.

Grenier, J. C., Ea, N., Pouchard, M. and Hagenmuller, P. (**1985**). "Structural Transitions at High Temperature in $Sr_2Fe_2O_{5,}$" J. Solid State Chem. **58**, 243-252.

Hodges, J. P., Short, S., Jorgensen, J. D., Xiong, X., Dabrowski, B., Mini, S. M. and Kimball, C. W. (**2000**). "Evolution of oxygen-vacancy ordered crystal structures in the perovskite series $Sr_nFe_nO_{3n-1}$ (n=2, 4, 8, and ∞), and the relationship to electronic and magnetic properties," J. Solid State Chem. **151**, 190-209.

Le Toquin, R., Paulus, W., Cousson, A., Prestipino, C. and Lamberti, C. (**2006**). "Time-resolved in situ studies of oxygen intercalation into $SrCoO_{2.5}$, performed by neutron diffraction and X-ray absorption spectroscopy," J. Am. Chem. Soc. **128**, 13161-13174.

Lindberg, F., Svensson, G., Istomin, S. Ya., Aleshinskaya, S. V. and Antipov, E. V. (**2004**). "Synthesis and structural studies of $Sr_2Co_{2-x}Al_xO_5$, $0.3\leq x\leq 0.5$," J. Solid State Chem. **177**, 1592-1597.

Liu, Y., Withers, R. L. and Fitz Gerald, J. D. (**2003**). "A TEM, XRD, and crystal chemical investigation of oxygen/vacancy ordering in $(Ba_{1-x}La_x)_2In_2O_{5+x}$, $0\leq x\leq 0.6$," J. Solid State Chem. **170**, 247-254.

Markov, A. A., Savinskaya, O. A., Patrakeev, M. V., Nemudry, A. P., Leonidov, I. A., Pavlyukhin, Yu. T., Ishchenko, A. V. and Kozhevnikov, V. L. (**2009**). "Structural features, nonstoichiometry and high-temperature transport in $SrFe_{1-x}Mo_xO_{3-\delta}$," J. Solid State Chem. **182**, 799-806.

Momma, K. and Izumi, F. (**2011**). "VESTA 3 for three-dimensional visualization of crystal,

https://doi.org/10.1017/S0885715613001152 Published online by Cambridge University Press

volumetric and morphology data," J. Appl. Crystallogr. **44**, 1272-1276.

Nakayama, N., Takano, M., Inamura, S., Nakanishi, N. and Kosuge, K. (**1987**). "Electron microscopy study of the "cubic" perovskite phase $SrFe_{1-x}V_xO_{2.5+x}$ ($0.05 \leq x \leq 0.1$)," J. Solid State Chem. **71**, 403-417.

Proffen, T. and Neder, R. B. **(1997**). "DISCUS, a Program for Diffuse Scattering and Defect Structure Simulations," J. Appl. Crystallogr. **30**, 171-175.

Takeda, Y., Kanno, K., Takada, T., Yamamoto, O., Takano, M., Nakayama, N. and Bando, Y. (**1986**). "Phase relation in the oxygen nonstoichiometric system, SrFeOx ($2.5 \leq x \leq 3.0$)," J. Solid State Chem. **63**, 237-249.

Weiss, M. (**1998**). *Reaktivität perowskitischer übergangsmetalloxide bei niederen temperaturen* (Mensch and Buch Verlag. Berlin).

https://doi.org/10.1017/S0885715613001152 Published online by Cambridge University Press